Appl. Phys. A 79, 453–456 (2004)
DOI: 10.1007/s00339-004-2665-3

Applied Physics A
Materials Science & Processing

W.D. YU✉
X.M. LI
X.D. GAO
P.S. QIU
W.X. CHENG
A.L. DING

Effect of zinc sources on the morphology of ZnO nanostructures and their photoluminescence properties

State Key Laboratory of High Performance Ceramics & Superfine Microstructure,
Shanghai Institute of Ceramics, Chinese Academy of Sciences, Shanghai 200050, P.R. China

Received: 28 January 2004 / Accepted: 4 February 2004
Published online: 16 March 2004 •

ABSTRACT The morphology and photoluminescence properties of ZnO nanostructures synthesized from deferent zinc sources by a vapor deposition process were investigated. The zinc sources involved pure zinc, ZnO, and $ZnCO_3$ powders, respectively. It was found that the zinc sources have a strong effect on the morphology of the ZnO nanostructures. For the pure zinc and ZnO sources, uniform ZnO nanowires and tetrapods are obtained, respectively. However, in the case of the $ZnCO_3$ source, the products are nanowire–tetrapod combined nanostructures, in which ZnO nanowires grow from the ends of tetrapod arms. The morphology differences of these products may be mainly concerned with the yield and constituents of the corresponding zinc vapor. Photoluminescence measurements show that the nanowires have a relatively stronger near-band UV emission than the other products. The strongest green-light emission from the tetrapods implies that more defects exist in the tetrapods. An evident peak at 430 nm is found in the spectrum of the nanowire–tetrapod combined nanostructures, which may be caused by oxygen-depletion interface traps.

PACS 73.61.Tm; 81.10.Bk; 78.55.Et

1 Introduction

One-dimensional (1-D) semiconductor nanomaterials have been attracting increasing attention due to their exceptional properties, which are different from bulk materials. In recent years, ZnO with wide direct band gap (3.37 eV) and large exciton binding energy (60 meV) is of great interest for electronic and photonic applications. Different fabrication methods, such as the AAO (Aluminium Anodic Oxide) template method [1], the vapor-transfer process [2–8], thermal evaporation [8–12], MOCVD (Metal Organic Chemical Vapor Deposition) [13–15], and hydrothermal synthesis [16, 17] have been widely reported for the preparation of simple 1-D ZnO nanostructures (nanowires, nanorods, nanobelts, etc.) and complex ZnO nanostructures (tetrapod-like, hierarchical, dendritic, etc.). Among them, the vapor-deposition method, involving the vapor-transfer process and thermal evaporation, is the most frequently used method. The experimental temperatures and the constituents of the zinc vapors produced in both processes are very different. In the vapor-transport process, the zinc source is a mixture of ZnO and graphite powders; the zinc vapor is produced by the carbothermal reduction of the ZnO powder under higher temperature ($> 900\,^{\circ}C$). The obtained vapor flow is a mixture of Zn (ZnO_x) vapor, CO_2 (CO), and carrier gas (Ar or N_2) [4]. However, in the evaporation method, the zinc source is a pure zinc powder. A lower temperature ($> 419\,^{\circ}C$, the melting point of Zn) is needed to vaporize Zn powder. The flow is just a mixture of pure zinc vapor and carrier gas.

On the other hand, for the production of high-quality ZnO nanowires, catalysts, such as Au [2, 3, 5], Cu [18], and NiO [10], etc., have been commonly used. The catalysts can improve the controllable growth of ZnO nanostructures. Here, we report success in synthesizing different ZnO nanostructures on Au catalyst substrates. Zn, ZnO, and $ZnCO_3$ powders were selected as the zinc source materials, respectively, to study the effects of the vapor yield and constituents on the morphology of ZnO nanostructures. Compared with commercial ZnO powder, $ZnCO_3$ powder can provide highly active ZnO powder by its pyrolysis, which results in a higher yield of the zinc vapor at relatively low temperature ($\sim 830\,^{\circ}C$). The room-temperature photoluminescence properties of the obtained materials were also investigated.

2 Experimental

ZnO nanostructures were synthesized in a horizontal tube furnace by a vapor-deposition method. Zinc sources were pure Zn powder, commercial ZnO powder (particle diameter ~ 100 nm, 99.99%) and basic $ZnCO_3$ powder (amorphous, 99%), respectively. Graphite powder (particle diameter $\sim 30\,\mu$m, 99%) was selected as a reducing agent. Si substrates were coated with Au films of around 5-nm thickness by a magnetron sputtering process on a LEYBOLD Z550 installation. The sources were placed at the center of the furnace, which was ramped to $900\,^{\circ}C$. The substrates were put in the temperature region of $600\,^{\circ}C$. Ar gas with a flow rate of 500 sccm was introduced

✉ Fax: +86-21/5241-3122, E-mail: ywd2003@mail.sic.ac.cn

as carrier gas. All deposition times were 15 min. The obtained products were characterized with field emission scanning electron microscopy (FESEM, JSM-6700F), transmission electron microscopy and selected-area electron diffraction (TEM/SAED, Philips FEI-CM200), and photoluminescence (UV-310, UV-VL spectroscopy, Xe lamp, 325 nm).

3 Results and discussion

Figure 1a shows that highly uniform ZnO nanowires were synthesized from the ZnO source. The diameters and lengths of the ZnO nanowires are less than 80 nm and up to several hundred micrometers, respectively. The inset shows a line of ZnO nanowires that was fabricated on the line of the Au film. It implies the catalysis of the Au film in our process. However, in the case of the pure zinc source, uniform ZnO tetrapods were obtained, as shown in Fig. 1b. The average diameters and lengths of the needle-like tetrapod arms were approximately 100 nm and 600 nm, respectively. Furthermore, ZnO nanowire–tetrapod combined nanostructures were synthesized from the $ZnCO_3$ source, as shown in Fig. 1c. The tetrapod arms are prismatic ZnO nanorods rather than needle-like nanorods [8, 19, 20]. The lengths of the most combined nanowires are several to several tens of micrometers, which are much longer than that produced formerly [20]. These nanowires (diameters of ~ 45 nm) are uniform, much thinner, and longer than the tetrapod arms, as shown in the inset of Fig. 1c.

The microstructures of ZnO nanowires and tetrapods have been widely investigated previously [2, 8, 19, 21, 22]. Similar results were also obtained in this work. However, very few reports about their combined nanostructure were found [20]. Figure 2a shows the typical TEM image of an arm–nanowire junction in the combined nanostructures. The inset shows the tip of the nanowire. No catalyst was found, which means that the likely growth mechanism of the nanowires is vapor–solid (VS). Figure 2b shows a high-resolution TEM image of the arm in the junction, while the inset is its SAED pattern. The same results were also obtained from the other products, e.g. nanorods in the tetrapod-only products (pure zinc source), nanowires in the nanowire-only products (ZnO source) and complicated ZnO nanostructures ($ZnCO_3$ source). The observed lattice fringes indicate a single-crystalline structure of all aforementioned products. The spacing between two adjacent lattice

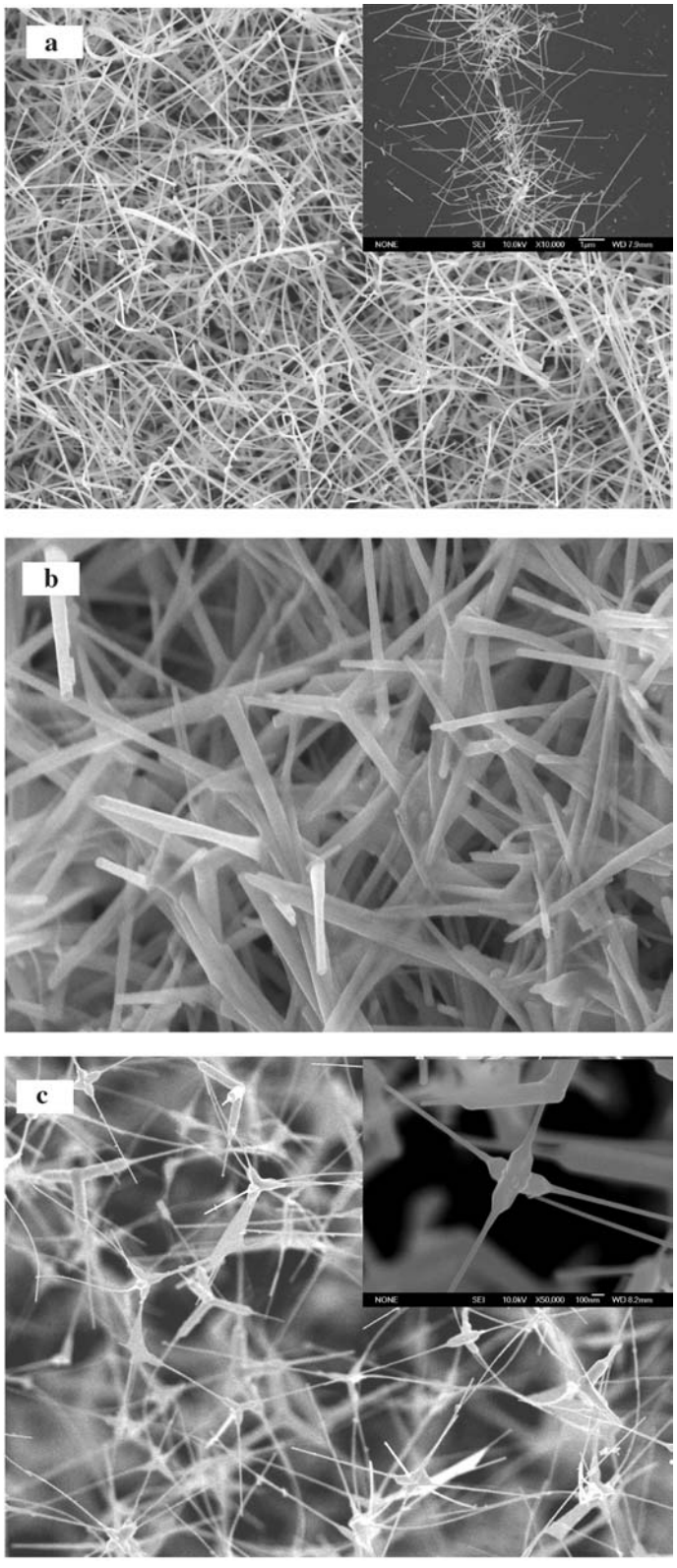

FIGURE 1 FESEM images of ZnO nanostructures obtained by using different zinc sources: **a** ZnO powder, the *inset* is the image of a nanowire line; **b** pure Zn powder; **c** $ZnCO_3$ powder, the *inset* is a magnified image of the nanowire–tetrapod combined nanostructures

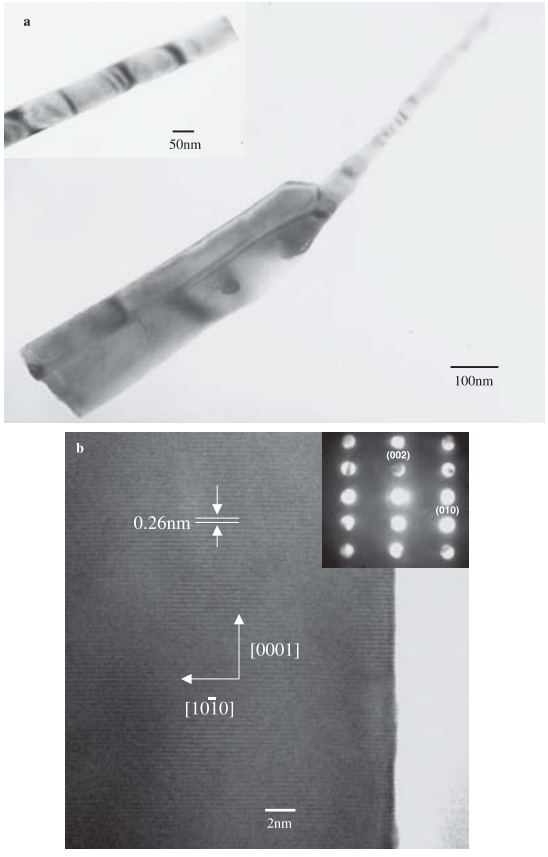

FIGURE 2 **a** A general TEM image of a nanowire–arm junction in the combined nanostructures. The *inset* is an image of the tip of the nanowire. **b** High-resolution TEM image of the arm in the junction. The *inset* is the corresponding SAED pattern

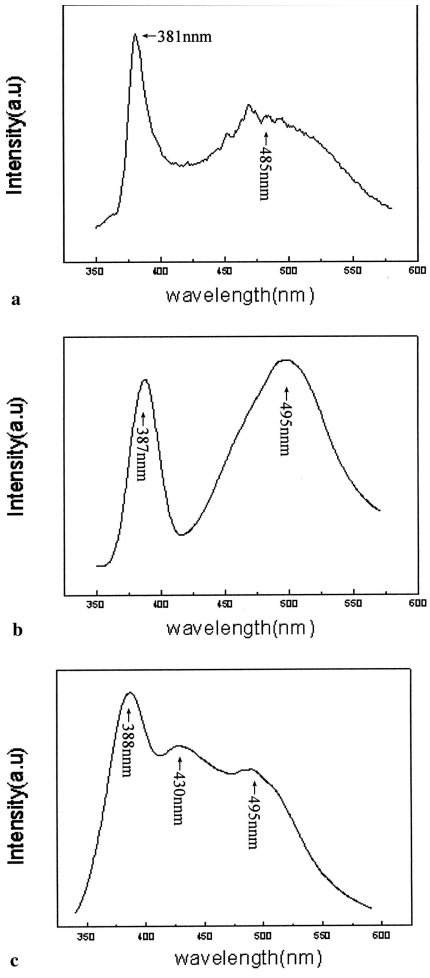

FIGURE 3 Photoluminescence spectra from the different ZnO nanostructures at room temperature: **a** nanowires, **b** tetrapods, **c** nanowire–tetrapod combined nanostructures

planes is about 0.26 nm, corresponding to the spacing of (002) planes in wurtzite ZnO crystal, and indicating growth along the [001] direction. These results are in agreement with the previous reports [2–17].

It is accepted that the ZnO nanowires formed in the present process were grown by the vapor–solid–liquid (VSL) mechanism [2, 3, 5] and the other products (tetrapods only and tetrapod–nanowire combined nanostructures) were grown by the VS mechanism [8, 19, 20]. All process parameters in this work are the same except for the zinc sources. Thus, it is reasonable to suggest that the morphology differences of these products may be linked to the use of different zinc sources. Due to the low melting point of Zn and highly active ZnO produced by decomposing basic $ZnCO_3$, the vapor yield from the pure zinc powder (Yz) is larger than that of $ZnCO_3$ (Yzc), and Yzc is larger than that from the ZnO powder (Yzo), namely Yz > Yzc > Yzo at the same temperature (900 °C). In addition, the compositions of the vapor flows from the three zinc sources are also different. In the case of the pure zinc powder, the flow is just a mixture of pure zinc vapor and carrier gas. However, for ZnO and $ZnCO_3$ powder, zinc vapor may be a mixture of Zn (ZnO_x), CO_2 (CO), and carrier gas [4]. So, for the pure zinc source, both necessary conditions of forming ZnO tetrapods, supersaturating zinc vapor and deficient oxygen gas, were satisfied. The catalysis of the Au film was eliminated entirely. On the contrary, in the case of the ZnO source, the yield of zinc vapor is too low to form ZnO tetrapods; the Zn (ZnO_x) vapor sufficiently reacted with the Au particles to grow ZnO nanowires. The formation of the nanowire–tetrapod combined nanostructures is complicated, which may be due to a concurrence of the above two processes. The high-yield zinc vapor was made for the nucleation of ZnO tetrapods. Then, due to more oxygen obtained from ZnO_x and CO_2, the growth of the arms of the tetrapods will be accelerated through simple chemical reactions as follows:

$$\mathrm{Zn(ZnO}_x\mathrm{)(g)} + \mathrm{CO_2(g)} \rightarrow \mathrm{ZnO(s)} + \mathrm{CO(g)},$$

$$\mathrm{ZnO}_x\mathrm{(g)} \rightarrow \mathrm{ZnO(s)} + \mathrm{Zn(g)}\,.$$

As the growing rate of (001) planes is larger than that of (100) planes [8], this acceleration may increase the aspect ratio of the tetrapod arms. Another fact that nanowires only formed at the ends of the tetrapod arms can also be interpreted by this mechanism.

Figure 3 shows the room-temperature photoluminescence of the ZnO nanostructures. Two luminescence bands, UV emission at 380–390 nm and green emission at 485–495 nm, were identified in all products. Similar results have been reported previously [2, 19, 20]. The relative intensity of UV emissions of nanowire-containing nanostructures (Fig. 3a and c) is larger than that of the tetrapods (Fig. 3b) and that reported by Dai et al. [19]. And, the relative intensity of the green-light peak from tetrapod-only products (Fig. 3b) is the largest. It may be caused by the fewer defects exist-

ing in ZnO nanowires synthesized by a high oxygen supply. The rapid formation of ZnO tetrapods from dense zinc vapor may produce many more defects. An obvious peak at around 430 nm was only found in Fig. 3c. According to Jin et al. [23], it may be due to the existence of oxygen-depletion interface traps in the ZnO_x film. In our work, ZnO_x particles may be formed in the growth of nanowire–tetrapod nanostructures. We believe that this violet emission is related to the remnants of these ZnO_x particles on the Au film.

In summary, the effect of zinc sources on the morphology of ZnO nanostructures has been investigated. This effect may be mainly concerned with the yields and constituents of the corresponding vapor flows. In the case of $ZnCO_3$, combined nanostructures, in which ZnO nanowires are grown directly from the ends of tetrapod arms, are synthesized. Two strong emissions at 380–390 nm and 485–495 nm, respectively, were observed from all products. The strongest green-light emission from ZnO tetrapods implies that more defects exist in the ZnO tetrapods. An evident peak at 430 nm is found in the spectrum of the combined nanostructures, which may be due to the existence of oxygen-depletion interface traps in the combined nanostructures.

ACKNOWLEDGEMENTS This project was financially supported by the National Natural Science Foundation of China (NSFC No. 50302013).

REFERENCES

1 Y. Li, G.W. Meng, L.D. Zhang, F. Phillipp: Appl. Phys. Lett. **76**, 2011 (2000)
2 M.H. Huang, S. Mao, H. Feick, H. Yan, Y. Wu, H. Kind, E. Weber, R. Russo, P. Yang: Science **292**, 1897 (2001)
3 M.H. Huang, Y.Y. Wu, H. Feick, N. Tran, E. Weber, P. Yang: Adv. Mater. **13**, 113 (2001)
4 B.D. Yao, Y.F. Chan, N. Wang: Appl. Phys. Lett. **81**, 757 (2001)
5 H. Ng, J. Li, M. Smith, P. Nguyen, A. Cassell, J. Han, M. Meyyappan: Science **300**, 1249 (2003)
6 J.Y. Lao, J.G. Wen, Z.F. Ren: Nano Lett. **2**, 1287 (2002)
7 P.X. Gao, Y. Ding, Z.L. Wang: Nano Lett. **3**, 1315 (2003)
8 H. Yan, R. He, J. Pham, P. Yang: Adv. Mater. **15**, 402 (2003)
9 B.Y. Geng, T. Xie, X.S. Peng, Y. Lin, X.Y. Yuan, G.W. Meng, L.D. Zhang: Appl. Phys. A **77**, 363 (2003)
10 S.C. Lyu, Y. Zhang, C.J. Lee: Chem. Mater. **15**, 3249 (2003)
11 H. Yan, R. He, J. Johnson, M. Law, R.J. Saykally, P. Yang: J. Am. Chem. Soc. **125**, 4430 (2003)
12 Z.W. Pan, Z.R. Dai, Z.L. Wang: Science **291**, 1947 (2001)
13 W.I. Park, D.H. Kim, S.-W. Jung, G.-C. Yi: Appl. Phys. Lett. **80**, 4232 (2002)
14 W.I. Park, G.C. Yi, M. Kim, S.J. Pennycook: Adv. Mater. **15**, 526 (2003)
15 J. Wu, S. Liu: Adv. Mater. **14**, 526 (2003)
16 L. Vayssieres: Adv. Mater. **15**, 464 (2003)
17 B. Liu, H.C. Zeng: J. Am. Chem. Soc. **125**, 4430 (2003)
18 S.Y. Li, C.Y. Lee, T.Y. Tseng: J. Cryst. Growth **247**, 357 (2003)
19 Y. Dai, Y. Zhang, Q.K. Li, C.W. Nan: Chem. Phys. Lett. **358**, 83 (2002)
20 V.A.L. Roy, A.B. Djurišić, W.K. Chan, J. Gao, H.F. Lui, C. Surya: Appl. Phys. Lett. **83**, 141 (2003)
21 M. Kitano, T. Hamabe, S. Maeda: J. Cryst. Growth **128**, 1099 (1993)
22 H. Iwanaga, M. Fujii, S. Takeuchi: J. Cryst. Growth **134**, 275 (1993)
23 B.J. Jin, S. Im, S.Y. Lee: Thin Solid Films **366**, 107 (2000)